Engineering Geology 335 (2024) 107529

Contents lists available at ScienceDirect

Engineering Geology

journal homepage: www.elsevier.com/locate/enggeo

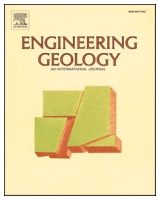

Seismic characterisation of the subsoil under a historic building: Cathedral Church of Saint Mary in Murcia case study

Marcos A. Martínez-Segura [a,*], María C. García-Nieto [a], Manuel Navarro [b], Marco D. Vásconez-Maza [c], Yoshiya Oda [d], Antonio García-Jerez [b], Takahisa Enomoto [e]

[a] Department of Mining and Civil Engineering, Universidad Politécnica de Cartagena, Paseo Alfonso XIII, 52, 30203 Cartagena, Spain
[b] Department of Applied Physics, University of Almería, 04120 Almería, Spain
[c] British Geological Survey, Nottingham, United Kingdom
[d] Tokyo Metropolitan University, Japan
[e] Department of Building Engineering, University of Kanagawa, Yokohama, Japan

ARTICLE INFO

Keywords:
Historical heritage
MASW
Mini-array
Seismic tomography
HVSR
3D Model
Amplification factor

ABSTRACT

This research focuses on the Cathedral Church of Saint Mary in Murcia, Spain, which is located in a moderate-to-high seismic risk zone in the Spanish context. The study uses geophysical techniques and geotechnical investigation to characterise seismic ground models at the building's scale, aiming to understand the real amplification of the ground under seismic effect in historic buildings. Three soil layers (silt, sand with gravel, and gravel) were identified through core borings. Multichannel Analysis of Surface Waves (MASW) profiles and Mini-array profiles revealed Vs values of 305 ± 32 m/s, 296 ± 62 m/s, and 440 ± 38.5 m/s, respectively, for these materials. Seismic Refraction Tomography (SRT) showed Vp values of 586 ± 73 m/s, 700 m/s, and 1466 ± 489 m/s for the corresponding layers. The horizontal-to-vertical spectral ratio (HVSR) approach identified a ground predominant period ranging from 0.37 to 0.38 s. Another significant peak at 2.3 s is observed, probably associated to the Triassic basement. Three seismic events with magnitudes Mw between 4.9 and 5.1 were used as inputs to determine the amplification factor (AF). The results indicate a PGA amplification factor between 1.7 and 2.1. These results contribute to the conservation and mitigation of seismic risk of this cultural heritage generating input data that enables precise computation of the soil-structure interaction.

1. Introduction

The vulnerability of historic buildings under seismic loads has been highlighted in numerous earthquakes, such as those that occurred in Axochiapan, Mexico (2007); Lorca, Spain (2011), and L'Aquila, Italy (2009). In countries with significant seismic activity, the protection and preservation of historical and architectural heritage represents a current and challenging problem (Hassan et al., 2020). Detailed knowledge of the type of building, the seismic response of the soil and the soil-structure iteration will allow the realisation of strategies aimed at intervention and the provision of solutions that guarantee the preservation of historic buildings (Falcone et al., 2021; Longobardi and Formisano, 2022).

Studies in urban areas showed that the existence of deposits of unconsolidated sedimentary materials can cause an increase in local seismic hazard (Vessia et al., 2021). Ground motion during an earthquake is modified depending on the type of materials through which it is transmitted, resulting in amplification or attenuation (Fabozzi et al., 2021). Amplification of the waves for certain frequency bands is caused by the contrast of velocities between the loose materials and the rigid basement. This phenomenon is known as site effect, being especially relevant when the amplification bands coincide with the natural period of existing buildings, causing the resonance effect (Martínez Segura et al., 2017).

The use of geophysical techniques to study the site effect is well known. Thus, seismic microzonation studies are carried out on a large scale (regional, local) to determine the seismic response of the ground to a seismic event. On a smaller scale, studies such as Grassi et al., 2021 carried out a geophysical campaign using different techniques to evaluate the dynamic characteristics of the Maniace Castle and its subsoil,

* Corresponding author.
E-mail addresses: marcos.martinez@upct.es (M.A. Martínez-Segura), mariacristina.garcia@edu.upct.es (M.C. García-Nieto), mnavarro@ual.es (M. Navarro), mvm@bgs.ac.uk (M.D. Vásconez-Maza), oda@tmu.ac.jp (Y. Oda), agj574@ual.es (A. García-Jerez), enomot01@kanagawa-u.ac.jp (T. Enomoto).

https://doi.org/10.1016/j.enggeo.2024.107529
Received 22 November 2023; Received in revised form 11 April 2024; Accepted 23 April 2024
Available online 24 April 2024

assessing the site resonance frequency and performing passive and active multi-channel surface wave analysis (MASW) surveys, while the horizontal standard spectral ratio (HSSR) and the random decrement method (RDM) techniques were used to obtain the dynamic properties of the structure. The subsoil beneath the San Michele Arcangelo Church and its environs were studied using ground penetrating radar (GPR), seismic refraction tomography (SRT), and MASW to determine the dynamic properties of the church building. To characterise the subsoil in terms of fundamental resonance frequency and amplification, horizontal-to-vertical spectral ratio (HVSR) measurements were taken at floor level, the various roof levels, and outside the building (Grassi et al., 2019). Giocoli et al., 2019 performed a study on the Orvieto Cathedral and its subsoil to obtain preliminary information useful for seismic assessment for a possible seismic event. For this purpose, the researchers investigate the surface geology and the foundation by means of electrical resistivity tomography (ERT) and the resonance frequency of the site by means of HVSR.

Due to the economic and social importance of historic buildings, a more detailed seismic study is required, specifically a building-scale seismic microzonation study. This research aims to obtain a seismic ground model at the scale of the building that allow us to know the real amplification of the ground under seismic effect. This will offer structural engineers actual dynamic soil data for the structural analysis of this building type. Thus, the geological and geotechnical characterisation was conducted on the basis of 7 core borings and laboratory tests. Five passive and active MASW profiles, 4 SRT profiles and 2 Mini-array profiles have been carried out for seismic characterisation. The HVSR of ambient noise has been also applied to obtain the predominant frequency of the ground.

Therefore, the objectives of the present work are: i) to define the different layers of material from the boreholes taken, ii) to seismically characterise each of the layers, iii) to obtain the ground velocity model, and iv) to estimate the seismic amplification factor (AF) and acceleration response spectrum (SA) of the site considering the ground surface conditions.

2. Study area and geological setting

2.1. Regional seismicity

Murcia city, with around 231,000 inhabitants and a 12.86 km^2 urban area surface, it is located in Murcia region (Southeastern Spain). This area belongs to the eastern part of the Betic region (Fig. 1), an Alpine chain placed at the westernmost part of the Eurasian and African Plates interaction zone (Sanz de Galdeano et al., 1995). This region is the most seismically active region in Spain, characterised by frequent earthquakes of small and moderate magnitude with moment magnitude (M_w) usually smaller than 5.5. However, historical seismicity data reveal that this region was affected by destructive earthquakes with epicentral macroseismic intensity with values of $I_0 \geq$ VIII in EMS-98 scale(European Macroseismic Scale, 1998) and calculated $M_w \geq 6.0$, among which we highlight the 1431 earthquake (Granada), 1522 (Almería), 1804 (Dalías, Almería), 1829 (Torrevieja, Alicante) and 1884 earthquake (Arenas del Rey, Granada) (Vidal, 1986; IGN, 2024).

Three seismic events of magnitude >6 have been recorded in the study area from 1900 onwards: the 1910 Adra (Almería) earthquake with body wave magnitude (m_b) = 6.2 (Stich et al., 2003), the 1954 Durcal (Granada) earthquake with m_b = 7.1 and 630 km deep (Chung and Kanamori, 1976) and the 2010 Granada earthquake with Mw = 6.2 and 650 km deep (Buforn et al., 2011). Most recently, several shocks

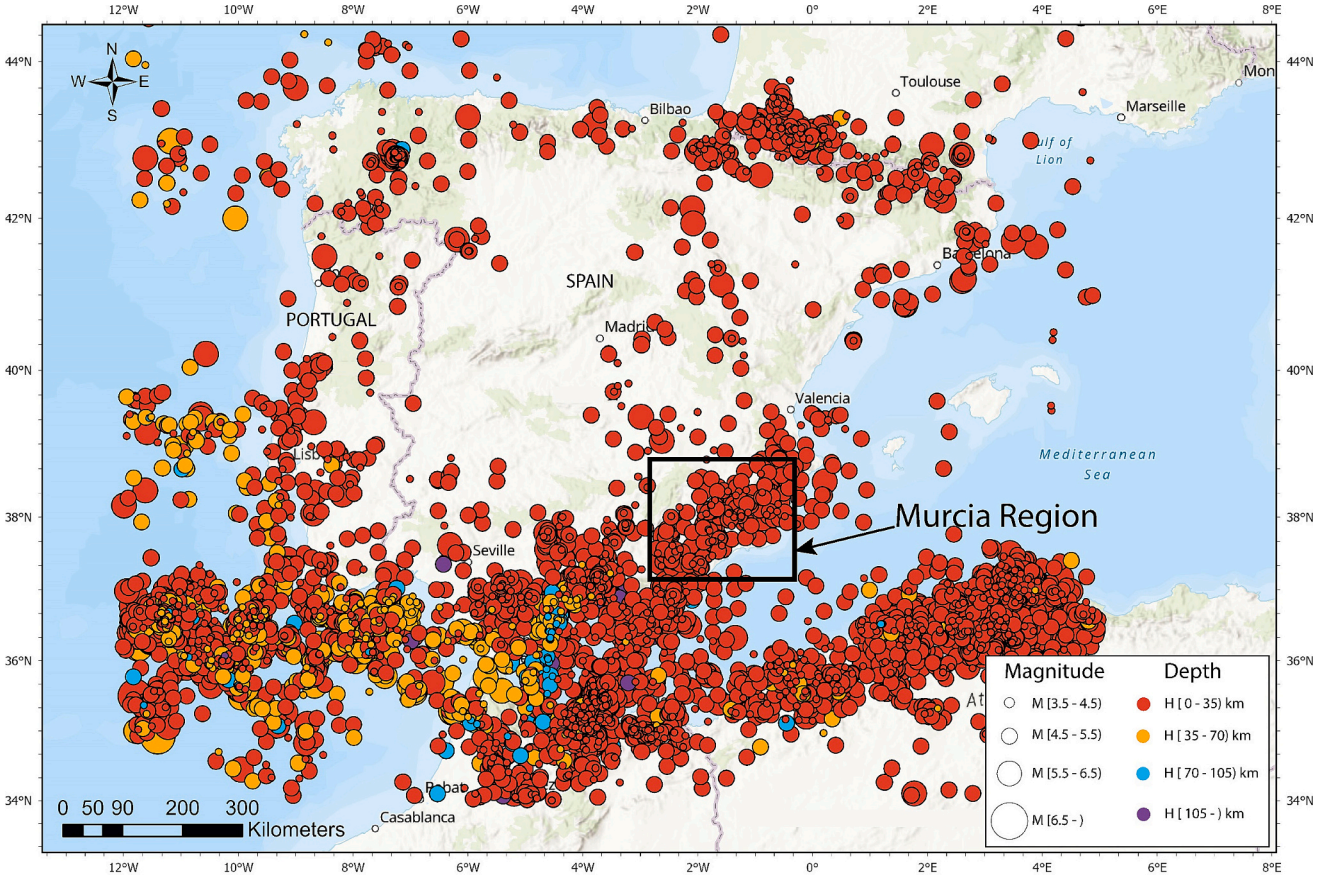

Fig. 1. Seismicity in the Iberian Peninsula taken from the IGN catalogue and updated until 2024 for earthquakes with magnitude >3.5 (IGN, 2024). The size of the marker indicates the magnitude of the earthquake while the colour the occurrence depth.

have occurred in the region during the last quarter century with Mw ≥ 4.5, such as the 1993 and 1994 Adra (Almería) earthquakes (Mw 4.9 and 5.0 respectively), the 1999 Mula (Murcia) earthquake (Mw 4.7), the 2002 Bullas (Murcia) earthquake (M_w 5.0), the 2005 La Paca (Murcia) earthquake (Mw 4.8) and the 2011 Lorca (Murcia) earthquake (Mw 5.2). These events have I_0 ranging from VI to VII on EMS-98 scale (IGN, 2024). Some of these events have shown the relevance of shallow geology for the explanation of both the ground motion amplification and the degree and spatial distribution of building destruction (García-Jerez et al., 2007; Navarro et al., 2014), highlighting the relevance of the features of the seismic ground response and its influence on building behaviour during the shaking.

Analysing the seismic catalogue of the Spanish National Geographic Institute (IGN, 2024), most of the seismic events have a shallow depth (h < 40 km), while a significant number have an intermediate depth (40 km < h < 150 km) and very few have a great depth (Buforn et al., 2011) (Fig. 1). The new seismic hazard map of Spain (IGN-UPM, 2013) reveals that this region has areas with expected peak ground acceleration (PGA) on rock >0.2 g for a 475-year return period, reaching 0.23 g in the city of Murcia.

2.2. Cathedral Church of Saint Mary in Murcia

The Santa Iglesia Catedral de Santa María, also known as the Cathedral of Murcia, is the architectural building par excellence of the city of Murcia (Fig. 2a). It is a construction located in the southeast of Spain of relevant historical and architectural interest, declared in 1931 an Asset of Cultural Interest, with the consideration of Monument. With a surface area of almost 5000 m^2, its construction began in the 14th century from the modification of a Muslim Mosque and throughout its history numerous interventions have been carried out, both for conservation and configuration (Vera Boti et al., 1994).

Located in an area of seismic risk, the historic earthquakes of 1716, 1732 and 1829 were particularly relevant in the generation of damage, with repairs being necessary in various areas, such as some of the church vaults, certain sculptures, and the lantern of the tower. Even the earthquake of 1732 aggravated the damage to the old façade of the church and its total demolition was considered necessary (Martínez Solares and Mezcua Rodríguez, 2002). The building complex has different architectural styles, due to its long construction period. Made of limestone masonry, it is composed of three main blocks, differentiated by their use and architectural form, such as the temple, the cloister, and the bell tower (Fig. 2b).

2.3. Geological setting

The area under study is located in the eastern sector of the Betic Cordillera. On a regional scale, two different Betic domains can be distinguished: a northern or external one and a southern or internal one. The first of these is subdivided into two different tectonic and palaeogeographic groups: the Prebetic, located in the outermost area, autochthonous, with shallow facies; and the Subbetic, overriding the former, allochthonous and with somewhat deeper facies. In the inner or Intrabetic domain, four superimposed structural complexes can be distinguished, more or less metamorphosed, from the Paleozoic Era. The innermost is the Nevado-Phyllabridean, which does not outcrop in the area; superimposed on this is the Ballabona-Cucharón, formed by slate, quartzite, gypsum and carbonates, tectonically over the previous one is the Alpujárride, composed of phyllites and quartzites, the highest complex tectonically is the Maláguide, outcropping in the Sierra de Carrascoy in the form of grauwacke, slates, pelites, carbonates and quartzites (Mulas de la Peña, 2015; Tessitore et al., 2015).

Murcia is located in the Guadalentín Depression delimited between two active fault systems. The Carrascoy Fault to the south and the Alhama de Murcia Fault to the north. This depression has a narrow and elongated shape with a general NE-SW direction and a variable elevation between 100 and 300 m formed by fills of Neogene-Quaternary materials, with locally important thicknesses, due to subsidence (Martín-Banda et al., 2016).

The Segura River flows into one of these subsidence pits, in a tectonic valley about 8–10 km wide, in a WSW-ENE direction, filled with Quaternary materials deposited by the river itself, fans and ejection cones of the encasing sierras. The sediments are detritic of all sizes, including clays and gravel, and can be up to 250 m thick, over silty loam deposits (Aragón et al., 2006) (Fig. 3).

The city of Murcia is in the floodplain of the Segura River (also known as the Vega Media of the Segura River), between the Contraparada (origin of the irrigation channel system of the Huerta) and the province of Alicante (Mulas de la Peña, 2015; Tessitore et al., 2015). The river flows through the plain, with a gradient of 5–6 m, forming closed meanders that have been artificially rectified at many points by means of walls, cuttings, channelling, etc. Four levels can be distinguished within the alluvial area of the city of Murcia: a first section formed by a shallow filling with a depth of between 0 and 15 m; followed by a second layer of clay and clayey or sandy silt with a depth of between 0.6 and 30 m; a third layer of silty sand and sandy silt with thicknesses between 1 and 14 m and, finally, a layer of gravel with thicknesses between 10 and 33

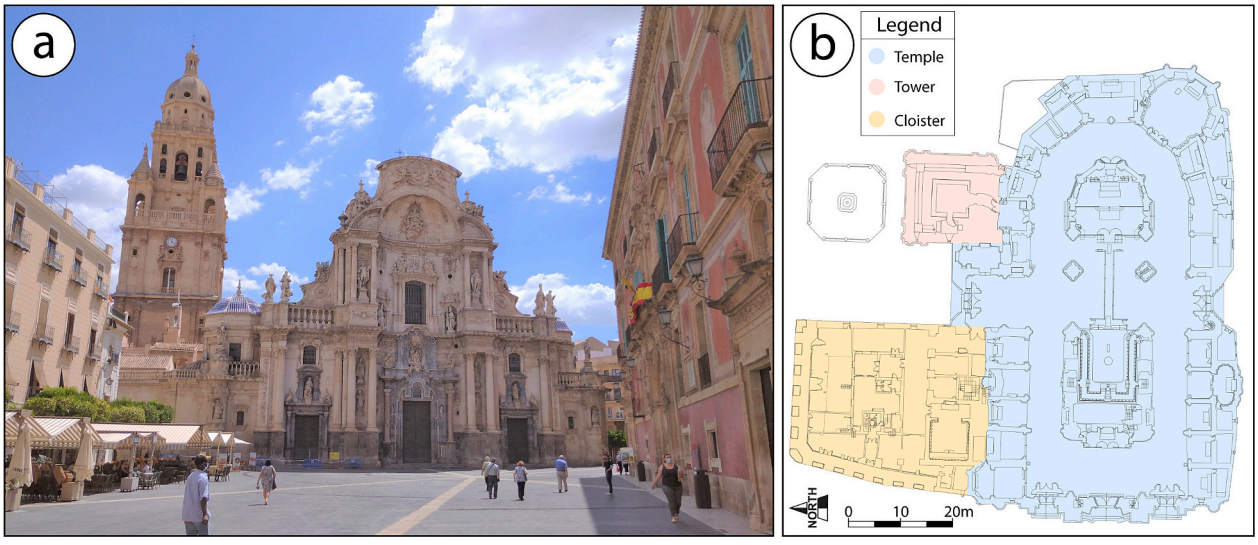

Fig. 2. a) West view of the Cathedral Church of Saint Mary in Murcia with its main frontage and the tower; b) Plan view of the main parts of the Cathedral.

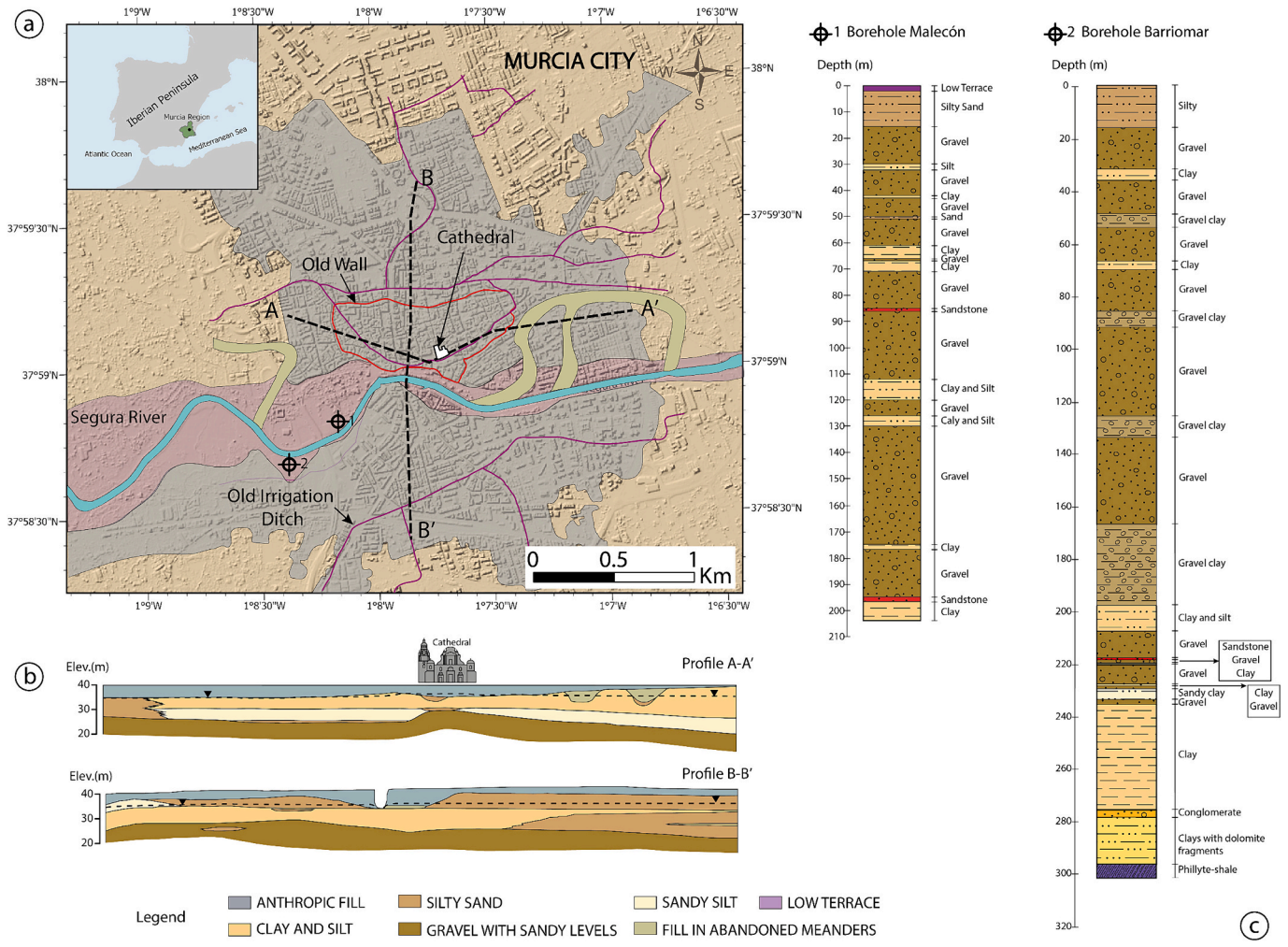

Fig. 3. a) Study area location and geological map of the surroundings of Murcia city (IGME/COPOT, 2001); b) Cross-sections A-A' and B-B′ (Mulas de la Peña, 2015); c) Stratigraphic column obtained from Malecón and Barriomar boreholes (Segura Hydrographic Confederation. Ministry of Environment Spain, 2024).

m.

There are specific areas of the urban area where this stratigraphic section is different from the previous one in its first few metres: such is the case of the areas immediately next to the riverbed, where there are significant thicknesses of fine saturated sand; in the abandoned meander of La Condomina, filled with looser and less consolidated silt than the surrounding area; the cava or ditch around the old wall, where the soil is also looser and there is a greater thickness of anthropic fillings; and in the vicinity of the old irrigation channels, where the soil is less consistent and, in general, has a sandier character, etc. (Mulas de la Peña, 2015) (Fig. 3a,b). The seismic basement can be associated to thick continuous layers of compact gravels (e.g. borehole 1 in Fig. 3c at about 70 m). Aragón et al. (2002) defined a high electrical resistivity basement in the Cathedral area at about 60 m below the ground level. Deep boreholes reached Triassic basement at a depth of about 300 m (see borehole 2 in Fig. 3c).

3. Available data

This section includes information stored in the Instituto de Patrimonio Cultural de España (IPCE. General Archive) concerning boreholes, laboratory and field tests carried out by the company Centro de Estudios, Investigación y Control de Obras, S.L. (CEICO, S.L.) at the request of the Spanish Ministry of Education and Culture. Directorate General of Fine Arts and Cultural Heritage. Institute for the Conservation and Restoration of Cultural Heritage.

Seven vertical boreholes (BH1-BH7) were drilled for a total of 158 m length (Fig. 4a). Thirty standard penetration tests (N_{SPT}), 19 unaltered samples and 2 hand samples for laboratory tests were conducted. Visual recognition and description of the samples, granulometric analysis and Atterberg limits were performed in order to identify and characterise the soil parameters. Simple compression tests to determine the geomechanical characteristics of the soil were also carried out. Together with the resistance to simple compression, the specific weight and natural humidity of the samples were obtained. Finally, Oedometric tests were performed to determine the compressibility of the soil.

4. Methodology

4.1. Estimation of shear wave velocity (Vs) from N_{SPT}

Vs of the surface sediments is the primary factor controlling the site effect. While direct determination of Vs through in-situ seismic methods and laboratory test is preferable, stablishing a reliable correction between Vs and penetration resistance would offer considerable advantages.

Many empirical correlations between uncorrected N_{SPT} and Vs have been described in the literature for particulate soils. Most studies use the functional form $Vs = AN^B$, where N is the 30 cm standard penetration tests value (N_{SPT}), and the constants A and B were determined by statistical regression of a data set. Correlations found in 24 different research works were summarized by Dikmen, 2009. Some other studies

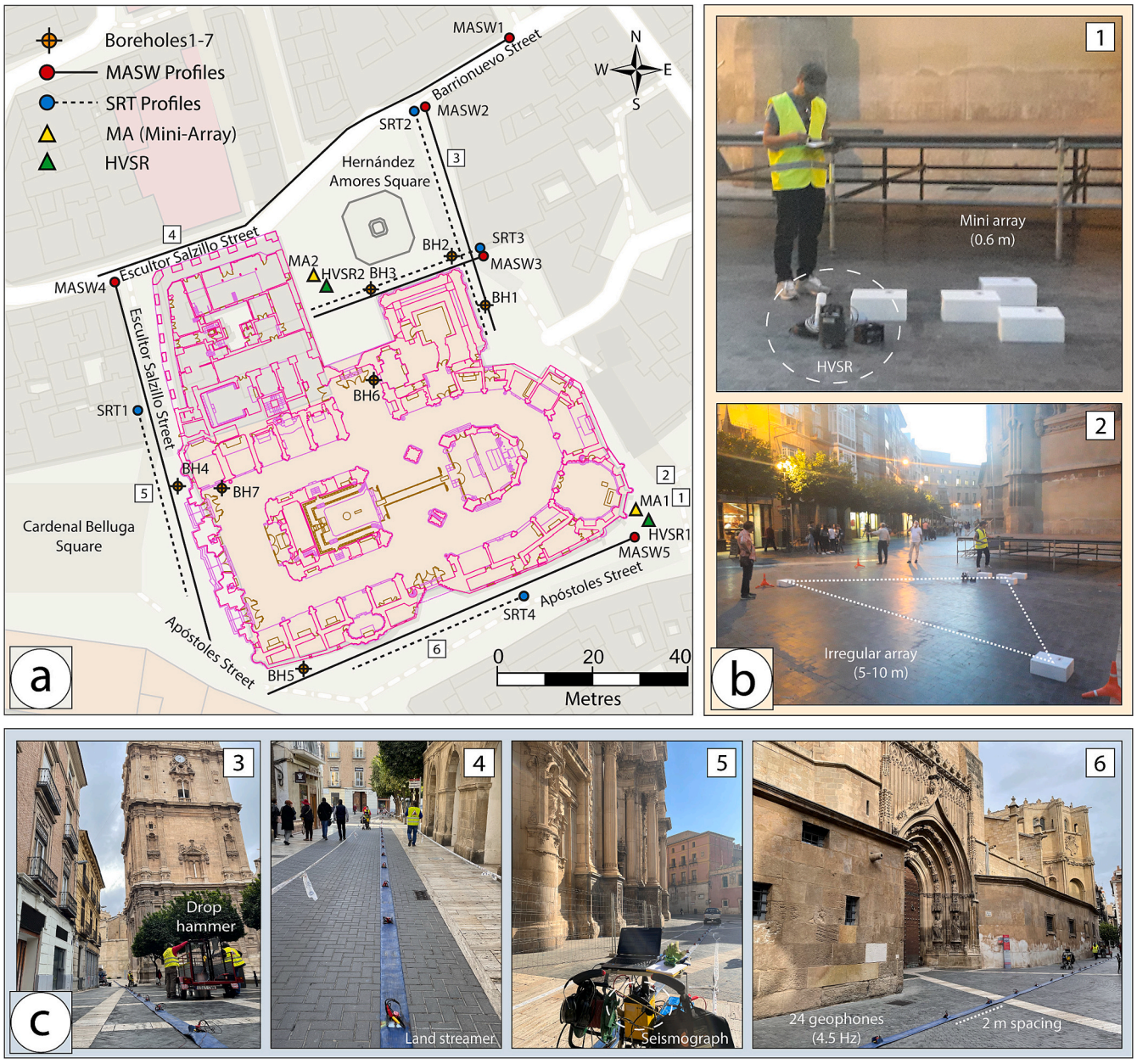

Fig. 4. Summary of field data collection. a) Positions of geotechnical and seismic surveys carried out at the Cathedral Church of Saint Mary in Murcia; b) HVSR and Mini-Array measurements: 1) Equipment; 2) Array setup and pictures of the measurements around the Cathedral; c) MASW and SRT measurements: 3) Drop hammer; 4) Land streamer; 5) Seismograph; 6) Equipment layout.

include the depth of material (h), which has an important influence in the resistant properties of soils, as an additional parameter together with N_{SPT} (Ohta and Goto, 1978; Alfaro, 2007). An empirical correlation between Vs, N_{SPT} and measurement depth was obtained for the metropolitan area of Madrid using 84 SPT test (Pérez-Santisteban et al., 2016). These equations have been summarized in Table 1.

Table 1
Some statistical correlations between N_{SPT} and Vs, including the depth of materials.

Author(s)	All soils	correlation coefficient
Ohta and Goto (1978)	$Vs = 61.62\ h^{0.222}\ N^{0.254}$	0.82
Alfaro (2007)	$Vs = 91.44\ h^{0.291}\ N^{0.298}$	0.46
Pérez-Santisteban et al. (2016)	$Vs = 71.05\ h^{0.382}\ N^{0.259}$	0.76

4.2. Geophysical data analysis

4.2.1. Mini-Array method

The Mini-Array method (Cho et al., 2013) is a technique to estimate the Vs structure from a microtremor measured by a miniature seismic array. The locations of the measurement points (the Hernández Amores Square and the Apóstoles Street) are just outside of the Cathedral (Fig. 4a, b). At each measurement point, we set six seismographs on the ground surface. One at the centre and three evenly spaced on a circumference of 60 cm radius (Mini-array). Other two seismographs were set on the ground surface 5–10 m apart from the centre seismograph (Irregular array). The seismographs used in this study were JU410 three-component accelerometers. The sampling rate and recording time were 200 Hz and 16 min respectively.

4.2.2. HVSR method

The HVSR method (Nakamura, 1989) was applied to obtain the predominant period of each site (Fig. 4a, b) by using two types of seismographs. One of them was similar to those used in Mini-array measurements and another one consisted of portable triaxial Güralp CMG-6TD seismometers to record the three components (North-South, East-West and Vertical) of ambient noise vibrations. A sampling frequency of 100 Hz and a recording time of 20 min were chosen for each point.

4.2.3. MASW method

The MASW surveys (Xia et al., 1999, 2000) were conducted in the outer areas surrounding the Cathedral, consisting of 5 profiles with a total of 406 m (Fig. 4a, c). The possibility of performing linear transects of lengths >60 m enabled the use of a land streamer equipment being designed to carry out continuous transects on the pavement without causing damage to it. In all the profiles, the active and passive methods have been combined, obtaining study depths larger than 30 m. For the active method, a 50 kg weight (drop hammer) falling from a height of a metre and tapping on a Teflon plate was used. For the passive method, the environmental noise produced by traffic, movement of people and other activities characteristic of urban environments, which are quite important in the area where the Cathedral is located, was used as a seismic source.

The equipment used consisted of a multi-channel recording system (seismograph), called the SUMMIT II compact unit from DMT (Germany) and a land streamer consisting of a hose on which 24 4.5 Hz geophones are distributed at 2 m between geophones. It is a mobile system, dragged at one end by an all-terrain vehicle, with the seismic source at the other end in the case of the active method. In each of the profiles, measurements were taken with a short distance to the first geophone (offset) of 10 m, a stack of 3 shot records for each site.

4.2.4. Seismic refraction tomography method

An SRT survey was carried out in the outer areas surrounding the Cathedral and consisted of 4 profiles (SRT1-SRT4) with a total of 192 m (Fig. 4a, c). The same array setup and the same seismic source used for MASW were employed for SRT. In each of the profiles, 9 shots were carried out at stations spaced 6 m apart, which is equivalent to taking one shot every 3 geophones. Smooth inversion tomography relies on a physically feasible model of first-break propagation for P and S wave soundings. The 1D velocity-depth profiles along the seismic line automatically generated from traveltime seismic data by horizontal averaging of the Delta-t-V method constituted an initial 1D model. Subsequently, a refined 2D model was obtained by applying 100 iterations of wavepath eikonal traveltime inversion (Schuster and Quintus-Bosz, 1993).

4.3. Amplification factor and acceleration response spectrum

The soil amplification factor in terms of peak ground acceleration (PGA) is defined as the ratio between the PGA values obtained in the seismogram recorded on the surface (PGA_S) and that corresponding to the recording at a reference site (PGA_R).

$$FA = \frac{PGA_S}{PGA_R} \quad (1)$$

To estimate the amplification factor due to ground surface conditions, the PGA values of the north-south (N-S) horizontal component of the reference earthquake and the simulated surface record, obtained from the convolution between the previous record and the ground model at each site, were compared.

For this purpose, we computed the ground motion acceleration of the shallow structure obtained at Hernández Amores Square and Apóstoles Street, which were chosen as calculation points. Three seismic events with magnitudes Mw between 4.9 and 5.1 corresponding to the main-shocks of the seismic series occurred in Adra (1993–1994) and Lorca (2011) were selected as input. These events were recorded at the strong motion stations of the national seismic network (IGN, 2024), located on bedrock outcrops composed mainly of schists, quartzites and phyllites. These earthquakes may be regarded as representative of the expected seismicity in the study area. In fact, for the city of Murcia, earthquakes with the greatest contribution to the seismic hazard for a return period of 475 years are those of moderate magnitude, ranging from 4.5 to 5.0 Mw, and a small source-to-site distance, between 0 and 10 km (SISMIMUR, 2006).

We used version 9.1 of Degtra A4 software (Ordaz and Montoya, 2012), which performs linear analysis of shear wave propagation in a 1-D stratigraphy with viscoelastic properties by the Thompson-Haskell method. To perform the calculation, it is necessary to provide the shear wave velocity, mass density, damping ratio and thickness for each one of the strata that make up the soil column. It is assumed that the stratigraphic column overlies an elastic half-space, whose properties must also be provided. Additionally, it is necessary to establish the angle of incidence. In our case, the analysis has been conducted using SH waves with an angle of incidence of zero (vertical incidence). Then, the simulated ground motion acceleration was computed by convolving the input accelerograms with the response of each 1-D model (Fig. 5), and the AF is calculated by dividing the PGAs of the simulated seismogram by the PGA of the input.

Finally, as a way to characterise the shaking severity of the simulated waveforms, the acceleration response spectrum (SA) has been computed via Duhamel's integration (also implemented in Degtra A4). The SA response represents the maximum absolute acceleration of damped single degree of freedom (SDOF) oscillators with different free periods T.

5. Results

5.1. Geotechnical parameters from available data

Seven boreholes were drilled achieving a depth range from 17 until 34.90 m. Analysis of the stratigraphic columns of the boreholes and the results of the laboratory tests are shown in Table 2.

Due to the location of the building, the subsoil around the cathedral follows the pattern of the alluvial area of Murcia. As mentioned above, four levels can be distinguished: superficial filling, clay and clayey or sandy silt, silty sand and sandy silt, and finally, a layer of gravel. In this study, we found seven layers distributed as follows: a first layer of superficial filling, following by a layer formed by clayey and sandy silt, which reaches approximately 10–12 m deep with a soft to medium consistency, simple compressive strength values mostly between 0.25 and 0.5 kg/cm^2, $N_{SPT} < 9$, and a high compressibility, which seems to decrease with depth. Below this silt, there is a level of silty sand and sandy silt with gravel of variable compactness, depending on the proportion of gravel that it contains. Thus, we have N_{SPT} between 7 and 53, which gives an idea of the heterogeneity of this level. At a depth between 12 m and 16.30 m, there is a layer of sandy gravel with high compactness and N_{SPT} in the range between 20 and rejection, with a mean value of 35 and 40. Below these gravels, a series of silt and sand strata can be detected, with a very rigid consistency, as well as compact gravel, being very compact from a depth of approximately 30 m onwards. The materials below the first layer of gravel already have a high level of compactness, as shown by the N_{SPT} tests carried out on the gravel at the base of borehole BH1, which present rejection in the two tests conducted (Fig. 6a).

Between 1994 and 1996 the water table dropped by 8 m, causing relative settlements of 10–12 cm in buildings in the city of Murcia (Rodríguez Ortiz and Mulas de la Peña, 2002). Such was the concern for the stability of the Cathedral that, between August 1997 and April 2001, sequential monitoring of the oscillations of the water table was carried out using piezometers. The measurement showed that in four years there had been a drop of >5 m with respect to the initial conditions, establishing the piezometric level in April 2001 at a depth of >9.5 m (IPCE.

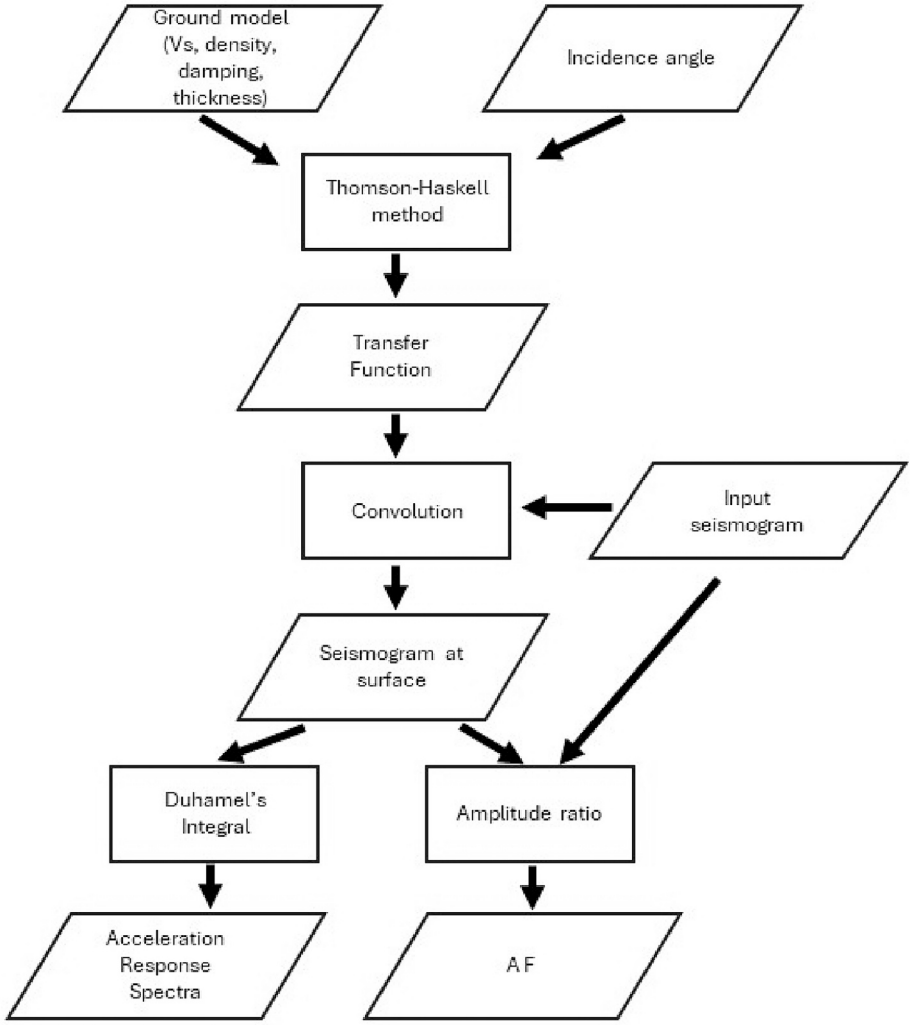

Fig. 5. Flowchart of ground amplification factor and SA response calculations.

General Archive). Due to the risk of possible liquefaction as the building is located on silty and sandy layers and the proximity of the Segura River, new measurements of the groundwater levels were carried out. The boreholes that allowed these measurements to be taken were BH6 and BH7. The results are shown in Table 3. The average depth of the piezometer was around 4 m with maximum centimetric variations found of 6 cm during the measurement period.

5.2. MASW surveys

The MASW was aimed at determining the shear wave velocities of each of the layers. The MASW1 (Fig. 4a) runs along Barrionuevo and Salzillo Streets. In the Barrionuevo Street, the mentioned three well-defined layers can be identified. The first one, with a depth of 12 m, shows velocity inversions (Fig. 6b). Thus, this layer can be subdivided into two sections, the first corresponding to the shallowest part down to ≈ 7.5 m, with shear wave velocities varying from 269 to 303 m/s, taking the average velocity of 285 m/s. The second section, between ≈ 7.5 m and 12 m with velocities of 228–268 m/s, is lower than the previous section. Then, from 12 m and ≈ 19 m velocity values between 457 and 499 m/s are shown taking the average velocity of 478 m/s. Finally, from 19 m onwards, velocity values >600 m/s. In Salzillo Street, three layers were also found: a surface layer with shear wave velocities ranging from 260 to 285 m/s down to 12 m, a second layer with an average Vs of 373 m/s down to 22 m, and a third layer with an average Vs of 459 m/s to the maximum depth of 30 m. Two profiles were conducted in the Hernández Amores Square (MASW2 and MASW3), where two layers were also detected: a layer with a Vs of 273 m/s down to 15 m, and a layer of higher Vs of 472 m/s to the maximum depth of 25 m. Three layers were found in the Cardenal Belluga Square (MASW4): a first layer with shear wave velocities ranging from 260 to 300 m/s down to 10 m, a second layer with a Vs of 358 m/s down to 13.3 m, and a third layer with an average Vs of 453 m/s to the maximum depth of 30 m (Fig. 6b). In Apóstoles Street (MASW5), two well-defined layers were found: a layer with a Vs of 293 m/s down to 12 m, and a layer with a Vs of 478 m/s to the maximum depth of 29 m.

5.3. Seismic refraction tomography

Just like the Vs values for the different layers of the subsurface, the Vp values have also been determined. Four SRT profiles (sites SRT1-SRT4) were conducted on the streets adjacent to the Cathedral (Fig. 4a). On the Salzillo Street and the Cardenal Belluga Square (SRT1), three layers were found: a variable silt layer, with a maximum thickness of 15 m in the area of the Escultor Salzillo Street, decreasing until it disappears from the main façade of the Cathedral (Cardenal Belluga Square) at velocities <600 m/s. This is followed by a second layer with velocities between 600 and 1500 m/s, more homogeneous between 15 and 23 m depth, which would correspond to the layer of sand and gravel. And, finally, a layer is shown from 23 m with velocities above 1500 m/s corresponding to the gravel layer. This layer cannot be correlated with the borehole as the borehole depth was ≈ 20 m.

Table 2
Results of the laboratory tests.

BOREHOLE	Depth (m)	Gravel (%) >5 mm	Sand(%) >0.08 mm	Fines(%) <0.08 mm	USCS*	AASHTO**	Compressive strength (kg/cm^2)	Bulk density (kg/cm^3)	Moisture Content (%)	Eoed *** (kg/cm^2)	Compression Index	Specific gravity
BH1	2.4–2.8	–	–	–	–	–	0.46	2.08	20.2	–	–	–
	6.0–6.6	0	6	94	CL	A-6(9)	0.22	2.01	26.3	–	–	–
	8.4–9.0	–	–	–	–	–	0.36	2.16	22.6	61	0.13	2.70
	10.8–11.4	–	–	–	–	–	0.46	2.12	22.6	–	–	–
	12.6–13.2	38	53	9	SP-SM	A-1a	–	–	–	–	–	–
	21.0–21.6	52	37	11	GP-GM	A-1a	–	–	–	–	–	–
	24.0–24.6	–	–	–	–	–	0.5	2.14	25.7	–	–	–
BH2	2.0–2.6	–	–	–	–	–	0.36	2.06	24.0	–	–	–
	4.2–4.8	–	–	–	–	–	0.30	–	–	–	–	–
	6.0–6.6	0	3	97	CL	A-6(15)	0.64	2.07	26.1	80	0.16	2.68
	8.4–9.0	–	–	–	–	–	0.26	2.17	24.3	–	–	–
	11.2–11.4	–	–	–	–	–	1.32	1.98	23.1	–	–	–
	11.4–12.0	0	28	72	ML	A-4(7)	0.42	2.04	24.5	72	0.14	2.69
	15.0–15.6	40	44	16	SM	A-1b	–	–	–	–	–	–
BH3	2.4–3.1	0	13	87	CL-ML	A-4(8)	0.61	2.00	22.0	96	0.15	2.67
	4.8–5.4	–	–	–	–	–	0.45	2.02	27.1	–	–	–
	8.3–8.9	0	44	56	ML	A-4(4)	–	–	–	–	–	–
	10.8–11.4	–	–	–	–	–	0.27	2.17	26.4	160	0.08	2.67
	18.0–18.6	64	29	7	GP-GM	A-1a	–	–	–	–	–	–
BH4	4.2–4.8	0	20	80	CL	A-4(8)	0.21	2.05	24.4	61	0.14	2.67
	6.0–6.6	–	–	–	–	–	0.15	2.10	25.9	–	–	–
	7.8–8.4	0	3	97	CL	A-6(8)	0.27	2.08	27.3	96	0.14	2.67
	11.4–12.0	0	40	60	ML	A-4(5)	–	–	–	–	–	–
BH5	5.5–6.1	0	30	70	ML	A-4(7)	–	–	–	–	–	–
	11.0–11.6	0	83	17	SM	A-2-4	–	–	–	–	–	–
	12.8–13.4	48	39	13	GM	A-1a	–	–	–	–	–	–
	23.7–24.0	–	–	–	–	–	0.73	1.97	24.8	–	–	–
	24.6–25.0	0	25	75	ML	A-4(8)	–	–	–	–	–	–

*Unified Soil Classification System; **American Association of State Highway and Transportation Officials; ***Oedometric Modulus.

Two profiles were conducted at Hernández Amores Square (SRT2-SRT3). The SRT2 profile reached a study depth of about 30 m where a first level of silt ≈ 6–10 m with velocities <600 m/s can be observed. Then there is a layer between 600 and 1500 m/s located ≈ 6–17 m deep, which can be correlated with the layer of sand and gravel. Finally, there is a layer with a higher velocity located from 17 m onwards with velocities of 1500 m/s, which can be associated with the gravel layer. It should be noted that from 20 m onwards, the velocity increases to values of over 2000 m/s, which could correspond to the more compact gravel package (Fig. 6d).

The SRT3 profile has reached ≈ 25 m deep, presenting 3 layers: a first layer located between the surface and the first 10 m with velocities between 200 and 600 m/s, corresponding to the silt layer. A layer located between 10 and 15 m deep, with a velocity between 600 and 800 m/s, being related to a layer of silty sand or gravel. Finally, a layer from 15 m deep with velocities of over 1000 m/s, corresponding to the gravel layer (Fig. 6d). Profile SRT4, conducted on Apóstoles Street, did not yield any results as the street is built on an old irrigation canal.

The profile SRT2 has been obtained with an error of 5.5%, which is equivalent to 4.44 ms after an inversion with 100 iterations at 50 Hz and a signal width of 10%. The profile shows velocities from 200 m/s to 2000 m/s. For better interpretation, the P-wave velocity isolines are highlighted in 250 m/s intervals.

5.4. Mini-Array method

The Rayleigh wave velocities and dispersion curves at the Apóstoles Street (MA1) and the Hernández Amores Square (MA2) estimated from microtremor data have been obtained. The phase velocities at the Apóstoles Street were more stable compared to the Hernández Amores Square. The dispersion curve at the Hernández Amores Square shows a frequency range from 6.8 to 48.0 Hz and phase velocities between 330 and 670 m/s. On the other hand, the dispersion curve at the Apóstoles Street shows a frequency range from 7.8 to 46.7 Hz and phase velocities from 270 to 525 m/s. The phase velocities obtained at the Hernández Amores Square are slightly higher than those obtained at Apóstoles Street. The shear velocity model at the Hernández Amores Square presents values of Vs between 344 and 756 m/s for a depth range between 3.8 and 50.3 m, whereas at Apóstoles Street, Vs ranges from 269 to 721 m/s for a depth from 3.6 to 36.8 m (Fig. 6c). The S-wave velocity up to 25 m depth at the Hernández Amores Square, north side of the Cathedral is a little higher than that of the Apóstoles Street (east side of the Cathedral). The average shear-wave velocity in the uppermost 30 m of the ground (V_{S30}) values at Hernández Amores Square and Apóstoles Street, estimated from the phase velocity at a wavelength of 40 m (Konno et al., 2000), are 450 m/s and 380 m/s respectively. According to these values, the grounds at these points are type II and III respectively under Spanish seismic code (NCSE, 2002) and class B according to Eurocode 8 (EC8) EN 1998–1 (2004) (Table 4).

5.5. HVSR method

The predominant period of the ground was determined from the spectral ratio between the geometric mean of the horizontal components and the vertical component of the ambient noise recordings (Fig. 4a). The results show that the maximum amplitude of the spectral H/V ratio at Hernández Amores Square (site HVSR2) corresponds to a period of 0.37 s (frequency 2.7 Hz) (Fig. 7). At Apóstoles Street (site HVSR1), the calculated predominant period is 0.38 s, with an associated frequency of 2.6 Hz (Fig. 7). A second dominant peak can be observed at low frequencies. It is especially clear at Apóstoles Street. This peak can be associated with impedance contrasts between deeper layers.

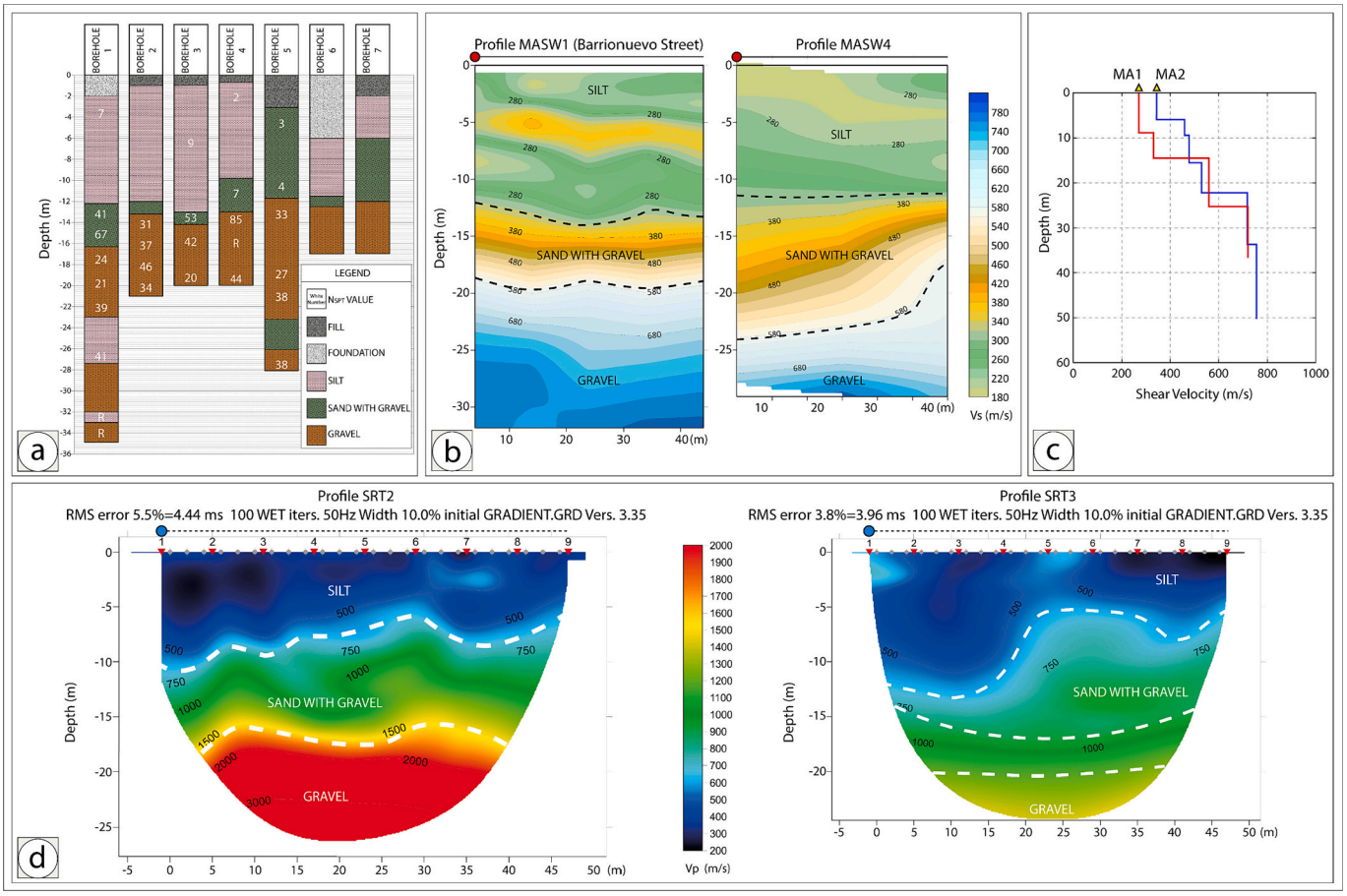

Fig. 6. a) Boreholes results: lithology around the Cathedral Church of Saint Mary in Murcia; b) MASW1 and MASW4 profiles: 2D sections of the shear velocities (Vs) obtained; c) Mini-Array measurements: Shear-wave velocity models obtained for the points located at Apóstoles Street (MA1 in red colour) and Hernández Amores Square (MA2 in blue colour); d) SRT2 and SRT3 profiles: 2D sections of the P-wave velocities (Vp) obtained. (For interpretation of the references to colour in this figure legend, the reader is referred to the web version of this article.)

Table 3
Piezometric results.

Borehole	Date	6/4/2021	11/25/2021	5/13/2022
BH6		4.2	4.11	4.07
BH7	Piezometric depth (m)	4.1	4.07	4.03

Table 4
Identification of ground types described on Eurocode-8 (EC8) and Spanish seismic code (NCSE, 2002).

Ground type		General description	V_{S30} (m/s)	
EC8	NCSE-02	Hard rock	EC8	NCSE-02
A	I	Medium hard rock	>800	>750
B	II	Hard soil and soft rock	360–800	400–750
C	III	Medium to soft soil	180–360	200–400
D	IV	Soft soil	<180	<200
E		Special soils	liquefaction	

6. Discussion

A complete characterisation of the elastodynamic properties of the subsurface structure provides a more reliable estimate of the seismic amplification of soils. For this, complementary geophysical techniques have been used in this work. SRT provided the V_P structure while MASW presents a high sensitivity to the V_S profile. An optimized common experimental setup allowed SRT and MASW measurements to be performed with high productivity. The mass density was determined from geotechnical tests. Microtremor array measurements using high-sensitivity seismometers and simulation of the HVSR of ambient noise, which is highly sensitive to impedance contrasts, allowed us to extend the Vs structure to higher depths, beyond the engineering basement.

The boreholes are in two areas, the first very close to the tower of the Cathedral (BH1, BH2, BH3, BH6) and the second in the opposite corner of the same, specifically on the Main Façade in the outside and inside the building (BH4, BH7) and, at the intersection of Apóstoles Street and Cardenal Belluga Square (BH5). The seismic profiles were arranged with two criteria, the first was to try to be as close as possible to the soundings and the tower and, secondly, to obtain information from all the streets surrounding the Cathedral (Fig. 4).

Mulas de la Peña, 2015 classified the soils of the city of Murcia into four type columns to obtain the response spectra. These columns were grouped according to soil types, characteristic thicknesses, Vs and specific weight (Table 5).

The results of the present study correspond to the type A column proposed by Mulas de la Peña, 2015, always taking into account average values (Table 5).

The calculation of velocities and thicknesses of the layer formed by infills has not been considered. This is because our main objective is to correlate the results of the different seismic techniques with the results of the boreholes. In this case, the geotechnical survey does not refer to the backfill layer. However, the thicknesses of this infill layer are negligible.

The second layer proposed by Mulas de la Peña, 2015, composed of

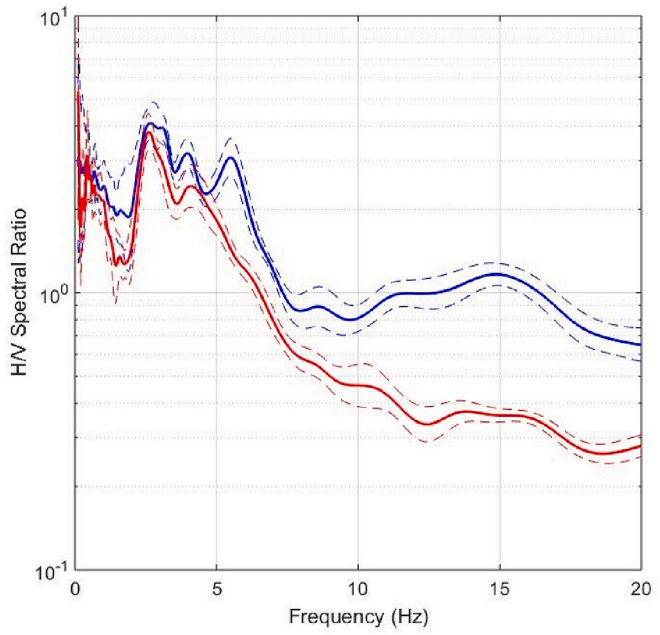

Fig. 7. H/V Spectral ratio at Hernández Amores Square (blue colour) and Apóstoles Street (red colour). Solid lines show mean values, and dashed lines limit one standard deviation intervals. (For interpretation of the references to colour in this figure legend, the reader is referred to the web version of this article.)

clay, silt and sand with a Vs = 270 m/s (type A), has been separated into two sublayers. The upper one composed of silt and clay and the lower one of sandy silt and silty sand. This subdivision was considered due to the presence of levels of gravels mixed with the sand which show a significant variation in geotechnical properties and shear wave velocity.

Silt and clay layer with a thickness of between 10 m and 12 m, according to the boreholes, and 9.3 ± 5.3 m, according to the geophysical campaign, of soft-medium consistency, compressive strength values mostly between 0.25 and 0.5 kg/cm^2, N_{SPT} < 9, and a high compressibility that seems to decrease with depth shows shear velocities are Vs = 305 ± 32 m/s and compressional wave velocities Vp = 586 ± 73 m/s. Layer of sandy silt and silty sand with variable thicknesses about 4 m, missing in some areas. It presents variable compactness depending largely on its gravel content; thus, we have N_{SPT} between 7 and 53, which gives an idea of the heterogeneity of this level. This is also shown by the values of Vs = 296 ± 62 m/s and Vp = 699 m/s.

The first layer of sandy gravel, with variable thicknesses ≈ 11.5 m, appears from 16 m in the boreholes and from ≈ 15 m in the geophysics campaign. The standard penetration test values are between 20 and rejection, and a typical value of approximately 35-40 can be adopted. This allows to deduce a relative density of about 40%, an internal friction angle of about 34° and a deformation modulus of about 500 kg/cm^2. In this layer, values of Vs of about 440 ± 39 m/s were found, similar to the Vs reported by Mulas (440-460 m/s). Values of Vp of 1470 ± 490 m/s were obtained.

The materials located below the first layer of gravel already present a high compactness, as shown by the values of the SPT carried out, with the gravel located at the base of borehole BH1, where rejection was obtained in the two tests conducted.

Table 6 compares, for three materials, the thicknesses, the average N_{SPT} values, the Vs values estimated from N_{SPT} (relationships in Table 1), the MASW and Mini-array Vs models, and the SRT Vp model recovered from two adjacent locations surrounding the Cathedral: Hernández Amores Square and Apóstoles Street (Fig. 6). It should be noted that the gravelly sand layer appears and disappears, with variable thicknesses and Vs values depending on the gravel content of the layer. In these two measurements, the layer made up of sand with gravel was not found.

The estimated Vs values show a higher standard deviation than the values measured with the MASW and Mini-array methods, highlighting the discrepancy when averaging relationships obtained in different geological settings. However, the average relative variation between estimated and measured values is <10%.

The comparison between Vs values from MASW and Mini-array reveals a similar trend in the silty sediments up to a depth of 12.9 m, 305 and 361 m/s in Hernández Amores Square with values of 293 ± 17 and 277 m/s in Apóstoles Street. It is followed by a layer of gravel with sand with higher velocity: 437 and 427 ± 26 m/s in Hernández Amores Square and 478 ± 21 and 336 ± 43 m/s in Apóstoles Street, respectively.

The Vp values at these two stations could not be compared because no results were obtained at Apóstoles Street. Velocities of 586 ± 73 m/s for the silt layer and 1470 ± 490 m/s for the gravel and sand were measured at depths of 12.9 and 25 m, respectively.

Based on the above results, a 3D velocity model of the subsoil of the Cathedral Church of Saint Mary in Murcia (Fig. 8) has been made. The model shows an upper layer formed by backfill that has been considered continuous, both inside and outside the Cathedral. However, the actual distribution underneath the Cathedral is unknown, because it may be part of the foundations or fillings that exist underneath the Cathedral and cannot be assimilated to the exterior areas.

Simulations of the HVSR from the underground structure using the diffuse field approach (García-Jerez et al., 2016; Sánchez-Sesma et al., 2011) suggest that the peak at 2.5–2.6 Hz is caused by an impedance contrast at a depth of about 63 m, beyond the range investigated by the performed seismic tests, with a stiffer layer of Vs ~ 1100 m/s (Fig. 9). The result is consistent with the Vs profiles of the study area obtained by Gestión del Subsuelo S.L. (unpublished results) by using passive MASW

Table 6
Layer thickness, Vp and Vs obtained from different methods

Layers	Thickness (m)	N_{SPT}	Vs (m/s) estimated from N-SPT	MASW Vs (m/s)	Mini-Array Vs (m/s)	SRT Vp (m/s)
Silt	9.3 ± 5.3	9	275 ± 83	305 ± 32	319 ± 42	586 ± 73
Sand with gravel	4.0 ± 4.0	30	300 ± 89	296 ± 62	–	699
Gravel	11.5 ± 3.5	37.5	440 ± 150	440 ± 39	416 ± 37	1470 ± 490

Table 5
Typical columns of the City of Murcia (Mulas de la Peña, 2015).

	A			B			C			D		
	Vs	h	Υ_W	Vs	h	Υ_W	Vs	h	Υ_W	Vs	h	Υ_W
Anthropic Fill	170	2.20	1.92	–			115	3.0	1.70	170	1.0	1.92
Clay, Silt and Sand	270	9.05	2.02	270	23.75	2.02	270	15.0	2.02	270	21.80	2.02
Gravel	460	–	2.35	460	–	2.35	460	–	2.35	460	–	2.35

Vs = Shear wave velocities (m/s); h = thickness (m); Υ_W = specific weight (t/m^2).

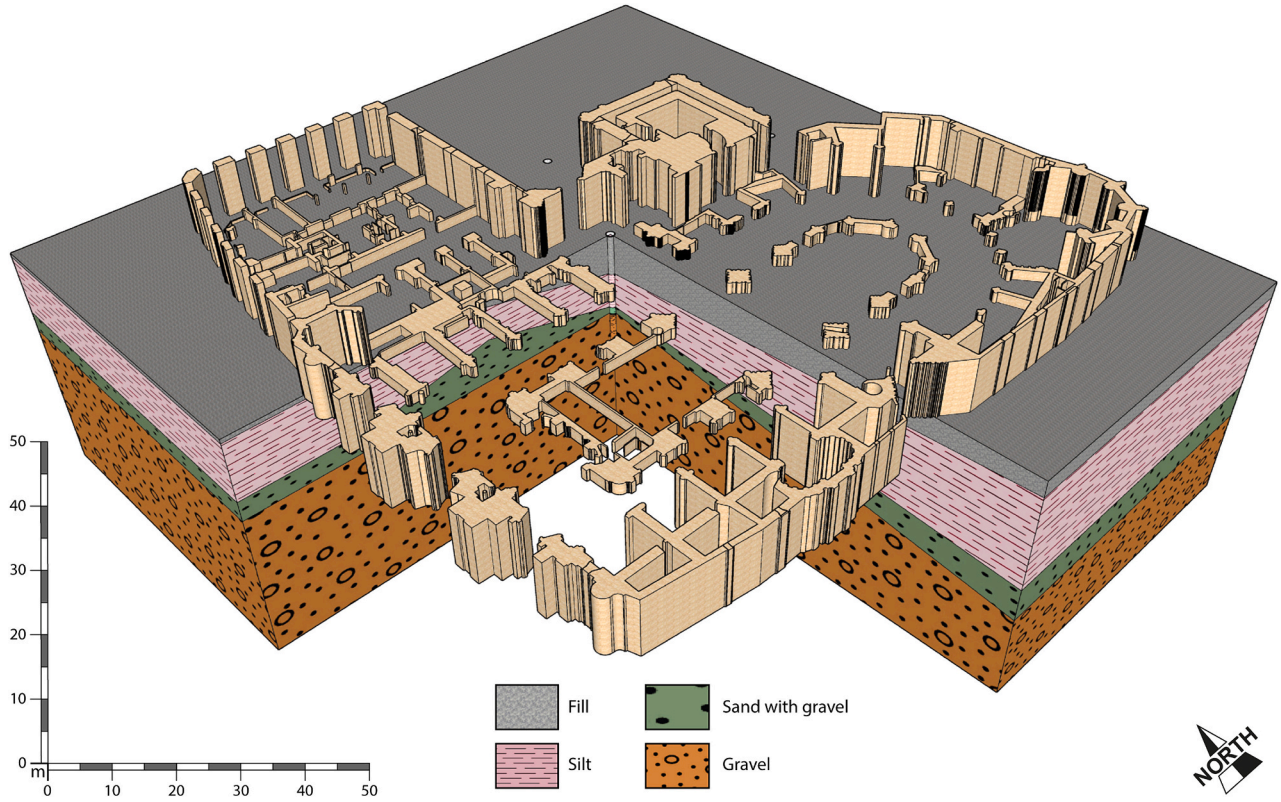

Fig. 8. 3D velocity model of the subsoil of the Cathedral Church of Saint Mary in Murcia.

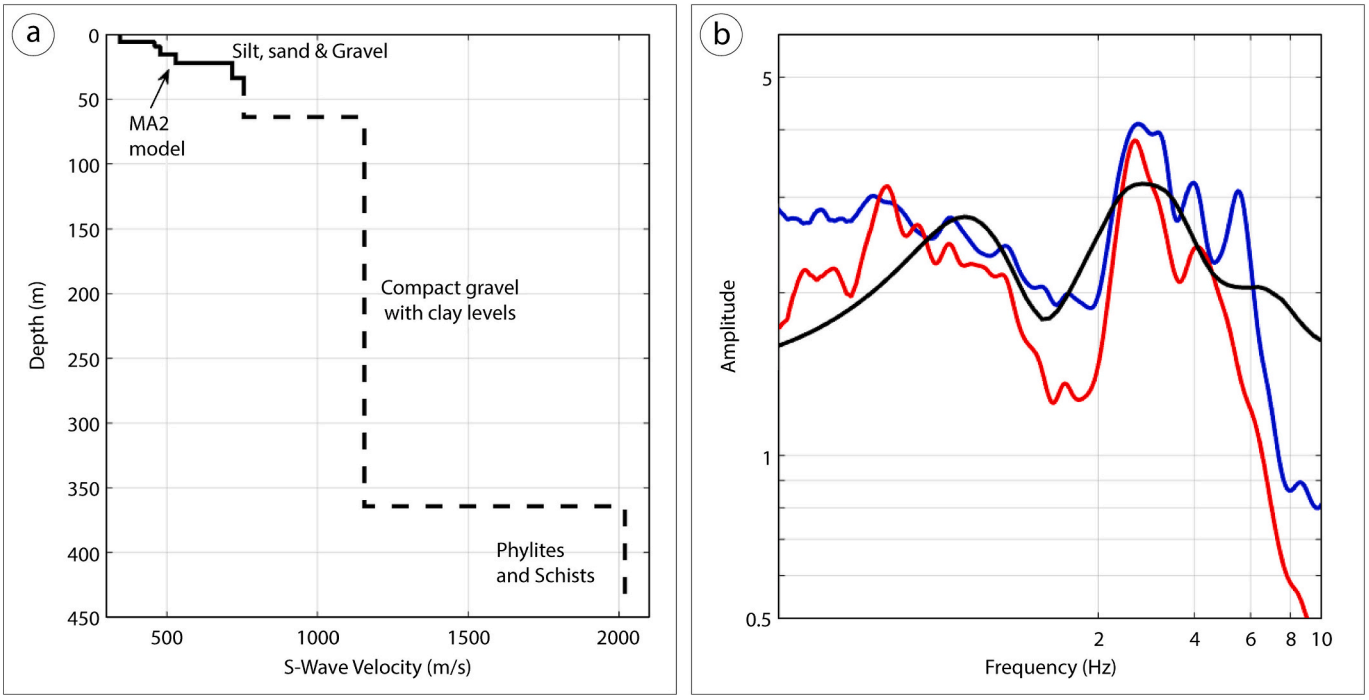

Fig. 9. Interpretation of the HVSR curve in the study area. (a) S-wave profile obtained at MA2 extended downwards from HVSR fitting; b) Experimental H/V curves at MA1 (red colour) and MA2 (blue colour) and simulated H/V (black line) for the model in panel (a). Stratigraphic interpretation of deepest layers is based on Borehole 2 (Fig. 3). (For interpretation of the references to colour in this figure legend, the reader is referred to the web version of this article.)

with 1 Hz geophones arranged in L-shaped arrays. This depth also matches well with the high electrical resistivity basement found in previous studies through the use of time domain electromagnetic (TDEM) surveys (see profile 7-SEDT in Aragón et al., 2002), corresponding to an impermeable layer that covers a thick formation of compact gravels (see borehole 1 in Fig. 3, as well as the interpretation of several boreholes in Murcia town and its surroundings, carried out by INYPSA, 2007). This layer can be considered as the seismic basement in

order to compute ground amplifications. Another velocity contrast is expected at about 350 m to reproduce the bump or broad peak found in the H/V below 1 Hz. That contrast can be attributed to the impermeable metamorphic basement of Triassic schists and phyllites described in a deep hydrogeological survey carried out 1.2 km SE of the Cathedral (Fig. 3c). Unfortunately, the density of sufficiently deep boreholes that reach these materials is scarce. Finally, peaks above 4 Hz are related to the shallow layering in the top 20 m.

The estimation of ground amplification factor will be of particular importance for the subsequent calculation of the soil-structure interaction for the Cathedral. Once the seismic-velocity ground model has been estimated, the ground amplification factor can be determined by dividing the PGA values of the simulated surface seismogram by the data sets used as input. These inputs have been applied at the engineering basement at 65 m depth (Fig. 9).

Fig. 10 shows the seismograms corresponding to the N-S components of the main earthquakes of the 2011 Lorca, and 1993 and 1994 Adra seismic series, recorded and simulated on the surface at Hernández Amores Square and Apóstoles Street. The respective SA responses for the horizontal components are compared in Fig. 11.

The mean amplification factor in PGA found for the horizontal components are 1.66 ± 0.11 at Hernández Amores Square and 2.11 ± 0.14 at Apóstoles Street. These results agree with the range of values obtained by Mulas de la Peña (2015) for the study area and are consistent with the expected amplification factors considering that the soils at these sites are type II and III respectively, according to the Spanish seismic code (NCSE, 2002). Note that the ground motion due to Lorca 2011 event, with horizontal peak ground acceleration reaching 0.37 g on rock site conditions and SA responses exceeding the design spectra of the Spanish seismic code for periods up to 0.5–1 s (Fig. 11) can be considered exceptional. Such high values have been explained by the combined result of a small epicentral distance (< 5 km), a very shallow hypocentral depth (4.6 km) and the effects of strong source directivity (Alguacil et al., 2014).

7. Conclusions

This article focuses on the detailed study of local effects in a historical building soil, the results of which are applicable to the analysis of the seismic risk of the monument. For this purpose, the seismic amplification of the soil around the Cathedral Church of Saint Mary in Murcia has been calculated.

The first step was to geologically and geotechnically classify the soil layers based on the results of the boreholes. The study revealed a stratified structure consisting of three layers in the upper 30 m. An upper layer of clayey silt with Vs = 305 ± 32 m/s and Vp = 586 ± 73 m/s. This is followed by a layer of sandy silt and silty sand with Vs = 296 ± 62 m/s and Vp value of about 700 m/s. Finally, a layer of sandy gravel with Vs = 440 ± 39 m/s and Vp = 1470 ± 490 m/s. A 3D model of this shallow structure has been obtained. V_{S30} values correspond to soils of category II-III (NCSE, 2002). A simplified model of the deeper structure, down to 300 m has been proposed.

Then, three seismic events with Mw magnitudes between 4.9 and 5.1 were used as input to estimate the amplification factor. The results reveal a PGA amplification in the horizontal components between 1.66 ± 0.11 and 2.11 ± 0.14. The variability in the results even in short distances emphasize the importance of performing detailed seismic site effect studies for heritage buildings.

The results of this study could be an important step forward in the correct seismic assessment in areas where the existing subsoil materials are prone to amplification, helping the preservation and risk reduction of existing cultural heritage structures through scientific and engineering knowledge. In this paper, we demonstrate how to provide input data that allows accurate calculation of the soil-structure interaction.

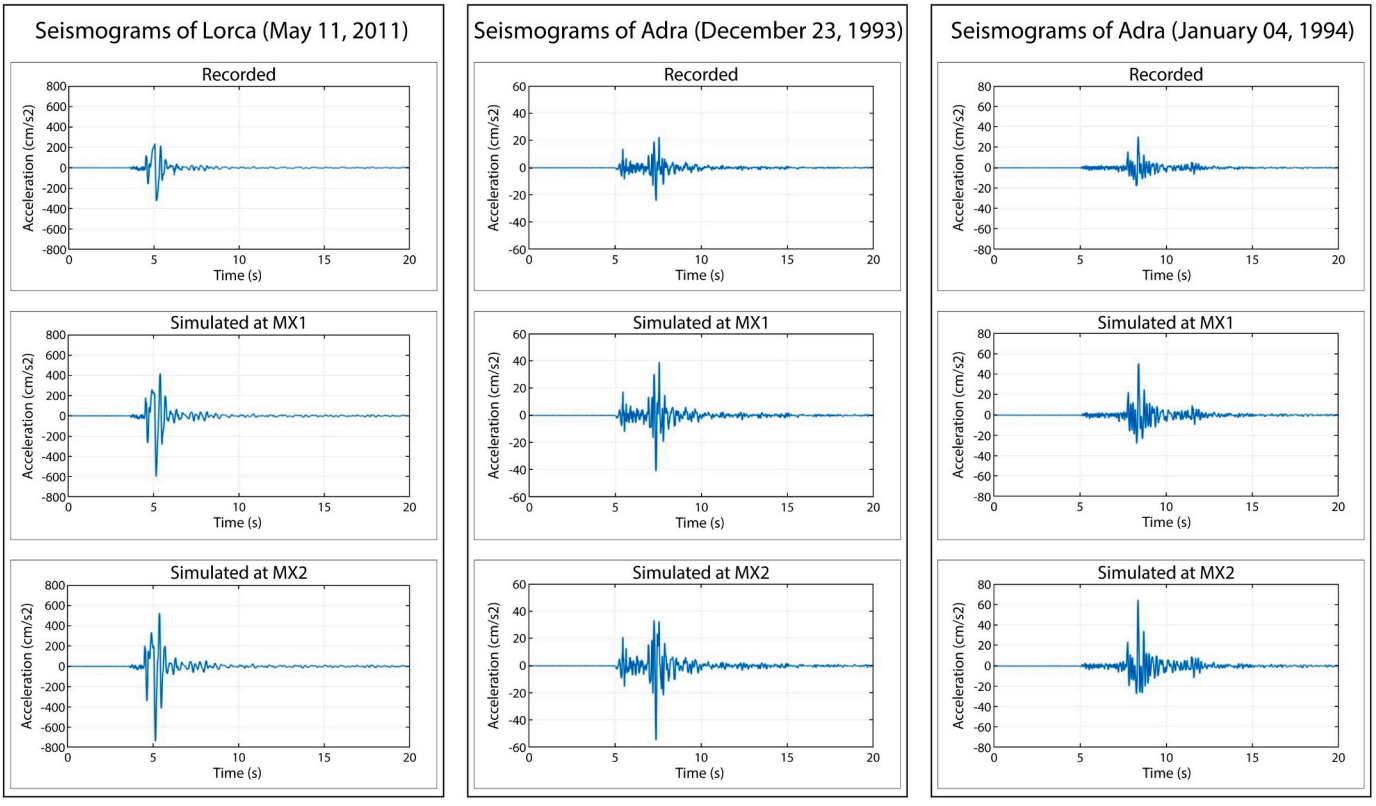

Fig. 10. Seismograms corresponding to the N-S components of the mainshocks of the 2011 Lorca, and the 1993–1994 Adra seismic series, recorded at rock sites and simulated at surface in Hernández Amores Square (MX1) and in Apóstoles Street (MX2).

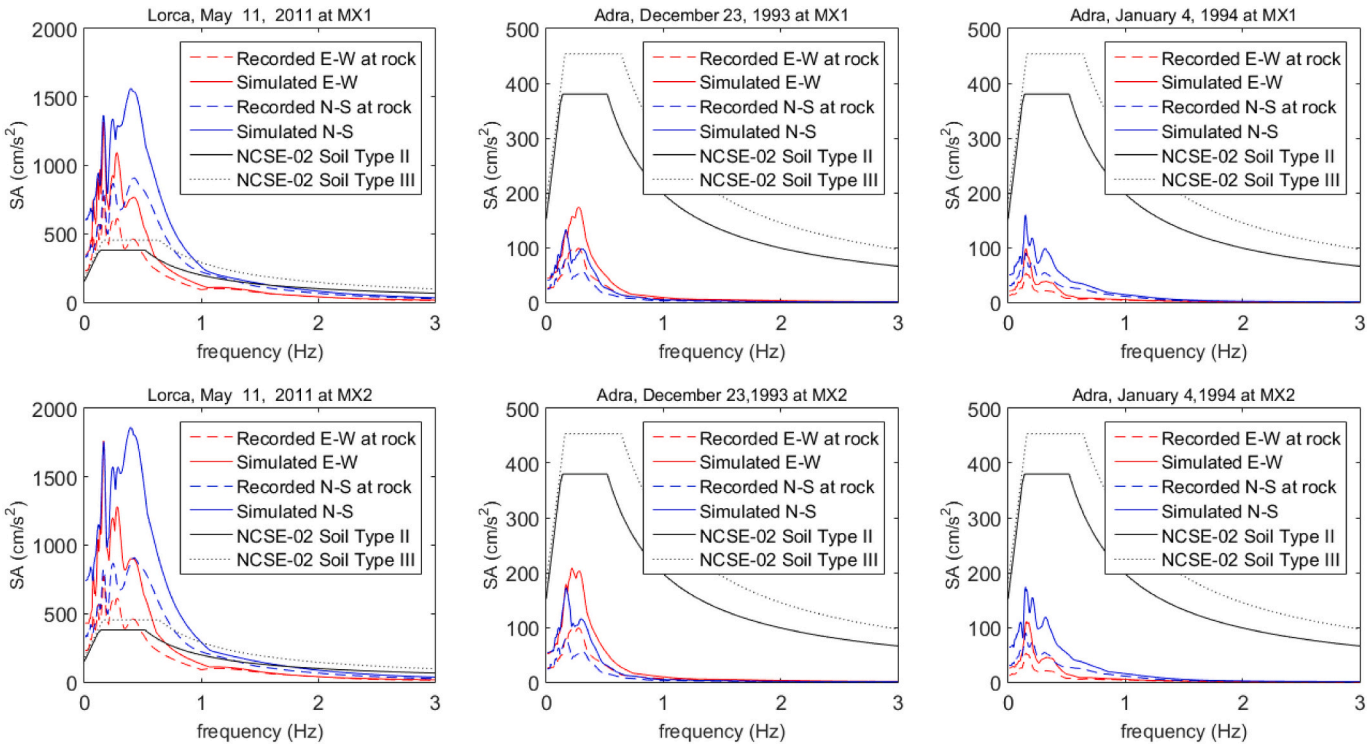

Fig. 11. SA response (5% damping) for the horizontal motion components of the 2011 Lorca, and the 1993–1994 Adra mainshocks, recorded at rock site and simulated at Hernández Amores Square (MX1) and Apóstoles Street (MX2). The results are compared to the design spectra prescribed by the Spanish seismic code (NCSE-02) for Murcia town on type II and type III soils.

CRediT authorship contribution statement

Marcos A. Martínez-Segura: Writing – review & editing, Writing – original draft, Visualization, Validation, Supervision, Software, Resources, Project administration, Methodology, Investigation, Funding acquisition, Formal analysis, Data curation, Conceptualization. **María C. García-Nieto:** Writing – review & editing, Writing – original draft, Visualization, Validation, Supervision, Software, Resources, Project administration, Methodology, Investigation, Funding acquisition, Formal analysis, Data curation, Conceptualization. **Manuel Navarro:** Writing – review & editing, Writing – original draft, Visualization, Validation, Supervision, Software, Resources, Methodology, Investigation, Formal analysis, Data curation, Conceptualization. **Marco D. Vásconez-Maza:** Supervision, Software, Investigation, Data curation. **Yoshiya Oda:** Validation, Software, Resources, Methodology, Investigation, Formal analysis, Data curation. **Antonio García-Jerez:** Writing – original draft, Validation, Software, Resources, Methodology, Investigation, Formal analysis, Data curation. **Takahisa Enomoto:** Validation, Software, Resources, Methodology, Investigation, Formal analysis, Data curation.

Declaration of competing interest

The authors declare that they have no known competing financial interests or personal relationships that could have appeared to influence the work reported in this paper.

Data availability

Data will be made available on request.

Acknowledgements

The authors thank the editor and the anonymous reviewers for their valuable comments which help to improve the manuscript. The Cathedral measurements were carried out thanks to the support of the «Project financed (21007/PI/18) by the Autonomous Community of the Region of Murcia through the call for aid to projects for the development of scientific and technical research by competitive groups, included in the Regional Programme for the Promotion of Research (Plan of Action 2019) of the Seneca Foundation, Science and Technology Agency of the Region of Murcia».

References

Alfaro, A., 2007. Correlación entre el Valor N del Ensayo de Penetración Estándar y Velocidad de Ondas de Corte para Arcillas en Bogotá - Colombia. Épsilon, 8, p. 3.

Alguacil, G., Vidal, F., Navarro, M., García-Jerez, A., Pérez-Muelas, J., 2014. Characterization of earthquake shaking severity in the town of Lorca during the May 11, 2011 event. Bull. Earthq. Eng. 12, 1889–1908. https://doi.org/10.1007/s10518-013-9475-y.

Aragón, R., Lambán, J., García-Arostegui, J.L., Hornero, J., Fernández-Grillo, A.I., Sánchez-Vidal, J.A., 2002. Estudio Hidrogeológico de la Unidad Vega Media y Baja del Segura. Vol XI. Ed. IGME, Madrid, Spain. In Spanish, 85 pp. Available at. http://info.igme.es/ConsultaSID/presentacion.asp?Id=80517.

Aragón, R., Lambán, J., García-Aróstegui, J.L., Hornero, J., Fernández-Grillo, A.I., 2006. Efectos de la explotación intensiva de aguas subterráneas en la ciudad de Murcia (España) en épocas de sequía: Orientaciones para una explotación sostenible. Bol. Geol. Min. 117 (3), 389–400.

Buforn, E., Pro, C., Cesca, S., Udías, A., Del Fresno, C., 2011. The 2010 Granada, Spain, deep earthquake. Bull. Seismol. Soc. Am. 101 (5), 2418–2430.

Cho, I., Senna, S., Fujiwara, H., 2013. Miniature array analysis of microtremors. Geophysics 78 (1). https://doi.org/10.1190/GEO2012-0248.1.

Chung, W.Y., Kanamori, H., 1976. Source process and tectonic implications of the Spanish deep-focus earthquake of March 29, 1954. Phys. Earth Planet. Inter. 13 (2), 85–96.

Dikmen, Ü., 2009. Statistical correlations of shear wave velocity and penetration resistance for soils. J. Geophys. Eng. 6 (1), 61–72. https://doi.org/10.1088/1742-2132/6/1/007.
Eurocode 8 (EC8) EN 1998–1, 2004. Design of structures for earthquake resistance Part 1: General rules, seismic actions and rules for buildings. Commission of the European Communities. Doc CEN/TC250/SC8/N335.
European Macroseismic Scale, 1998. Conseil de L'Europe. In: Grunthal, G. (Ed.), Cahiers du Centre Européen de Géodynamique et de Séismologie, 15. Luxembourg.
Fabozzi, S., Catalano, S., Falcone, G., Naso, G., Pagliaroli, A., Peronace, E., Porchia, A., Romagnoli, G., Moscatelli, M., 2021. Stochastic approach to study the site response in presence of shear wave velocity inversion: application to seismic microzonation studies in Italy. Eng. Geol. 280, 105914 https://doi.org/10.1016/j.enggeo.2020.105914.
Falcone, G., Acunzo, G., Mendicelli, A., Mori, F., Naso, G., Peronace, E., Porchia, A., Romagnoli, G., Tarquini, E., Moscatelli, M., 2021. Seismic amplification maps of Italy based on site-specific microzonation dataset and one-dimensional numerical approach. Eng. Geol. 289, 106170 https://doi.org/10.1016/j.enggeo.2021.106170.
García-Jerez, A., Navarro, M., Alcalá, F.J., Luzón, F., Pérez-Ruiz, J.A., Enomoto, T., Vidal, F., Ocaña, E., 2007. Shallow velocity structure using joint inversion of array and h/v spectral ratio of ambient noise: the case of Mula town (SE of Spain). Soil Dyn. Earthq. Eng. 27 (10), 907–919. https://doi.org/10.1016/j.soildyn.2007.03.001.
García-Jerez, A., Piña-Flores, J., Sánchez-Sesma, F.J., Luzón, F., Perton, M., 2016. A computer code for forward calculation and inversion of the H/V spectral ratio under the diffuse field assumption. Comput. Geosci. 97, 67–78. https://doi.org/10.1016/j.cageo.2016.06.016.
Giocoli, A., Hailemikael, S., Bellanova, J., Calamita, G., Perrone, A., Piscitelli, S., 2019. Site and building characterization of the Orvieto Cathedral (Umbria, Central Italy) by electrical resistivity tomography and single-station ambient vibration measurements. Eng. Geol. 260, 105195 https://doi.org/10.1016/j.enggeo.2019.105195.
Grassi, S., Imposa, S., Patti, G., Boso, D., Lombardo, G., Panzera, F., 2019. Geophysical surveys for the dynamic characterization of a cultural heritage building and its subsoil: the S. Michele Arcangelo Church (Acireale, eastern Sicily). J. Cult. Herit. 36, 72–84. https://doi.org/10.1016/j.culher.2018.09.015.
Grassi, S., Patti, G., Tiralongo, P., Imposa, S., Aprile, D., 2021. Applied geophysics to support the cultural heritage safeguard: a quick and non-invasive method to evaluate the dynamic response of a great historical interest building. J. Appl. Geophys. 189, 104321 https://doi.org/10.1016/j.jappgeo.2021.104321.
Hassan, H.M., Fasan, M., Sayed, M.A., Romanelli, F., ElGabry, M.N., Vaccari, F., Hamed, A., 2020. Site-specific ground motion modeling for a historical Cairo site as a step towards computation of seismic input at cultural heritage sites. Eng. Geol. 268, 105524 https://doi.org/10.1016/j.enggeo.2020.105524.
IGME/COPOT, 2001. Mapa Geológico de la Ciudad de Murcia a escala 1:2500.
IGN-UPM WORKING GROUP, et al., 2013. Actualización de mapas de peligrosidad sísmica de España 2012. Centro Nacional de Información Geográfica 267.
Instituto Geográfico Nacional (IGN), 2024. Catálogo de terremotos 2024. https://doi.org/10.7419/162.03.2022.
INYPSA, 2007. Nueva aportación al conocimiento hidrogeológico del entorno urbano de Murcia. In Spanish, Available at. https://www.chsegura.es/es/.
Konno, K., Kataoka, S.I., Konno, K., 2000. New method for estimating the average s-wave velocity of the ground. In: Proc. of the 6th International Conf. on Seismic Zonation.
Longobardi, G., Formisano, A., 2022. Seismic vulnerability assessment and consolidation techniques of ancient masonry buildings: the case study of a Neapolitan Masseria. Eng. Fail. Anal. 138, 106306 https://doi.org/10.1016/j.engfailanal.2022.106306.
Martín-Banda, R., García-Mayordomo, J., Insua-Arévalo, J.M., Salazar, Á.E., Rodríguez-Escudero, E., Álvarez-Gómez, J.A., Medialdea, A., Herrero, M.J., 2016. New insights on the seismogenic potential of the Eastern Betic Shear Zone (SE Iberia): Quaternary activity and paleoseismicity of the SW segment of the Carrascoy Fault Zone. Tectonics 35 (1), 55–75. https://doi.org/10.1002/2015TC003997.
Martínez Segura, M.A., Navarro Bernal, M., Martínez Pagan, P., 2017. Riesgos sísmicos en la Región de Murcia y métodos de evaluación de la peligrosidad sísmica a escala urbana. LOS RIESGOS AMBIENTALES EN LA REGIÓN DE MURCIA. Ediciones de la Universidad de Murcia, Murcia, pp. 35–37. ISBN 978-84-17157-45-6.
Martínez Solares, J.M., Mezcua Rodríguez, J., 2002. Catálogo sísmico de la Península Ibérica (880 a.C.-1900), vol. 18. Ministerio de Fomento. Subdirección General de Producción Cartográfica, Madrid (ISBN 84-95.172-37-2.).
Mulas de la Peña, J., 2015. Análisis de los aspectos geotécnicos en depósitos sedimentarios recientes con vistas a la microzonación sísmica. Aplicación a la ciudad de Murcia. Doctoral Thesis.. Universidad Politécnica de Madrid https://oa.upm.es/57753/.
Nakamura, 1989. A method for dynamic characteristics of surface. In: Proc. 20th JSCE Earthquake Eng. Symposium, Vol. 30, Issue 1, pp. 133–136.
Navarro, M., García-Jerez, A., Alcalá, F.J., Vidal, F., Enomoto, T., 2014. Local site effect microzonation of Lorca town (SE Spain). Bull. Earthq. Eng. 12 (5), 1933–1959. https://doi.org/10.1007/s10518-013-9491-y.
NCSE, 2002. Norma de Construcción Sismorresistente. Ministerio de Fomento, Real Decreto 997/2002 de 27 de septiembre. Boletín Oficial del Estado, 244, pp. 35898–35967.
Ohta, Y., Goto, N., 1978. Empirical shear wave velocity equations in terms of characteristic soil indexes. Earthq. Eng. Struct. Dyn. 6 (2), 167–187. https://doi.org/10.1002/EQE.4290060205.
Ordaz, M., Montoya, C., 2012. Programa DEGTRA A9 versión 9.1.0. Instituto de Ingeniería, Universidad Nacional Autónoma de México, México.
Pérez-Santisteban, I., Martin, A.M., Carbó, A., Ruiz-Fonticiella, J.M., 2016. Empirical correlation of shear wave velocity (Vs) with spt of soils in Madrid. Near Surf. Geosci. 1, 495.
Rodríguez Ortiz, J.M., Mulas de la Peña, J., 2002. Subsidencia generalizada en la ciudad de Murcia (España). Riesgos Naturales 459–463. ISBN 84–344–8034-4.
Sánchez-Sesma, F.J., Rodríguez, M., Iturrarán-Viveros, U., Luzón, F., Campillo, M., Margerin, L., García-Jerez, A., Suarez, M., Santoyo, M.A., Rodríguez-Castellanos, A., 2011. A theory for microtremor H/V spectral ratio: application for a layered medium. Geophys. J. Int. 186 (1), 221–225. https://doi.org/10.1111/j.1365-246X.2011.05064.x.
Sanz de Galdeano, C., López Casado, C., Delgado, J., Peinado, M.A., 1995. Shallow seismicity and active faults in the Betic Cordillera. A preliminary approach to seismic sources associated with specific faults. Tectonophysics 248 (3–4), 293–302. https://doi.org/10.1016/0040-1951(94)00279-I.
Schuster, G.T., Quintus-Bosz, A., 1993. Wavepath eikonal traveltime inversion: theory. SEG (Society of Exploration Geophysicists) 58 (9), 1314–1323. https://doi.org/10.1190/1.1443514.
Segura Hydrographic Confederation. Ministry of Environment Spain, 2024. Retrieved February 20. from. https://www.chsegura.es/es/.
SISMIMUR, 2006. General Directorate of Civil Protection, Civil Protection Special Plan to the Seismic Risk in the Region of Murcia, Annex 5. Department of the Presidency of the Region of Murcia, Spain.
Stich, D., Ammon, C.J., Morales, J., 2003. Moment tensor solutions for small and moderate earthquakes in the Ibero-Maghreb region. J. Geophys. Res. Solid Earth 108 (B3).
Tessitore, S., Fernández-Merodo, J.A., Herrera, G., Tomás, R., Ramondini, M., Sanabria, M., Duro, J., Mulas, J., Calcaterra, D., 2015. Regional subsidence modelling in Murcia city (SE Spain) using 1-D vertical finite element analysis and 2-D interpolation of ground surface displacements. Proceedings of the International Association of Hydrological Sciences 372, 425–429. https://doi.org/10.5194/piahs-372-425-2015.
Vera Boti, A., Sánchez-Rojas Fenoll, M.C., De la Peña Velasco, C., Pascual Martínez, L., Esbert Alemany, R.M., 1994. La Catedral de Murcia y su plan director (C. O. de A. de Murcia, Ed.).
Vessia, G., Laurenzano, G., Pagliaroli, A., Pilz, M., 2021. Seismic site response estimation for microzonation studies promoting the resilience of urban centers. Eng. Geol. 284 https://doi.org/10.1016/j.enggeo.2021.106031.
Vidal, F., 1986. Seismotectonics of the Region Betics-Alboran Sea. PhD thesis,. University of Granada (Spain).
Xia, J., Miller, R.D., Park, C.B., 1999. Estimation of near-surface shear-wave velocity by inversion of Rayleigh waves. Geophysics 64 (3), 691–700. https://doi.org/10.1190/1.1444578.
Xia, J., Miller, R.D., Park, C.B., Ivanov, J., 2000. Construction of 2D Vertical Shear-Wave Velocity Field by the Multichannel Analysis of Surface Wave Technique. In: Symposium on the Application of Geophysics to Engineering and Environmental Problems. Environment and Engineering Geophysical Society, pp. 1197–1206. https://doi.org/10.4133/1.2922726.